

ON THE PHOTOFISSION CROSS SECTIONS OF ^{209}Bi , ^{232}Th , and
 ^{238}U AT INTERMEDIATE ENERGIES (*)

by

H.G. de Carvalho, J.B. Martins and O.A.P. Tavares
Centro Brasileiro de Pesquisas Físicas
Rio de Janeiro, Brasil

and

V. di Napoli and M.L. Terranova
Istituto di Chimica Generale ed Inorganica dell'Università - Roma

(Received 25th October 1973)

ABSTRACT

Photofission cross sections have been estimated for ^{209}Bi , ^{232}Th and ^{238}U , in the energy range from 0.15 GeV up to 2 GeV, using fissility values computed with the Monte Carlo Method. For the calculation of the fissilities, use has been made of some already known results of proton-induced intranuclear cascade calculations, in

(*) Work supported by the Brazilian Conselho Nacional de Pesquisas, Comissão Nacional de Energia Nuclear and Banco Nacional do Desenvolvimento Econômico, and Italian Consiglio Nazionale delle Ricerche.

order to obtain information about mass number, atomic number and excitation energy distributions of the post-cascade nucleus. The calculation has been carried out as a fission-evaporation competition, using an energy dependence of the ratio of the neutron evaporation width to fission width. The results have been compared with experimental data, showing that the photofission cross sections are consistent with the photomeson mechanism of nuclear excitation.

I. INTRODUCTION

Fission is a frequent mode of nuclear de-excitation following the interaction of intermediate energy photons or particles with medium-heavy and heavy nuclei. Its contribution to the total inelastic cross section may be very large, or even predominant.

At incident energies in excess of about 100 MeV the particle-nucleus interaction model proposed by Serber¹ has been generally accepted. This model predicts a two-step reaction mechanism: a prompt cascade, which originates in the interaction of the incoming particle with a single nucleon within the target nucleus and leads to the ejection of a number of nucleons^(*), leaving an excited nucleus, and a second step, much slower, resulting in the evaporation of a relatively large number of particles from this excited nucleus. The nucleus arising from cascade

(*) Emission of light nuclides is also possible at this stage via the mechanism of fragmentation, which seems to occur on a time scale comparable with that of the fast nucleonic cascade.

my also de-excite in the second step by fission which competes with the evaporative processes at any stage of the evaporation. Both evaporation and fission treat the post-cascade nucleus as a whole.

In photon-induced reactions above 150 MeV, the production of pions plays a predominant role. The Serber model was developed by Reff² in such a way as to be fitted to these reactions and has been shown by different authors^(*) to explain the sudden increase of reaction cross sections above the pion photoproduction threshold. Another mechanism, however, has been proposed by Levinger³, which bases upon the assumption that the incoming photon is absorbed by a neutron-proton pair within the nucleus (the so-called "quasi-deuteron") at energies up to about 500 MeV. The photodisintegration of a quasi-deuteron would thus be the primary event, then followed by cascade and fission-evaporation competition.

Since fission must be regarded as a collective process in the nucleus, knowledge of the photofission cross section and nuclear fissility would lead to a better understanding of either nuclear structure or collective nuclear excitation.

Early in 1953, Bernardini et al.⁴ interpreted the remarkable increase in the photofission cross section of ^{209}Bi at energies in excess of 150 MeV, on the basis of pion photoproduction. Since then, a number of investigators have made contributions to the field of photofission, and the experimental data available at present for heavy and medium-heavy nuclei⁵⁻¹⁹ are sufficient to allow a systematic study. Moreover, due to the large errors involved in the measurements, there exist

(*) See for example, C.E. Roos and V.Z. Peterson, Phys.Rev. 124, 1610(1961).

large discrepancies among the cross section and fissility values obtained in different laboratories. Such discrepancies may be ascribed also to the different experimental methods employed in measuring the cross sections, the different values of the total inelastic cross section assumed in calculating the fissilities, the different interpretation of the primary interaction mechanism, and to other causes more difficult to evaluate.

The present work has been undertaken with the hope of explaining the general trend of photofission cross section at intermediate energies. For this purpose we carried out a Monte Carlo calculation of the fission-spallation competition during the evaporation step for the target nuclei ^{209}Bi , ^{232}Th and ^{238}U at photon energies ranging between 0.15 GeV and 2 GeV. We chose these three nuclei for the following reasons: first, the experimental data for these nuclei are more abundant in literature than the data available for other nuclei in the same mass region, and secondly, they have masses sufficiently different to allow a comparison between the results of the calculation.

II. THE PHOTOFISSION CROSS SECTION

For photon energies above the π -meson production threshold, the photofission cross section $\sigma_f(E)$ can be written in the form

$$\sigma_f(E_\gamma) = \left[A\sigma_o(E_\gamma) k(E_\gamma)\delta + L \frac{NZ}{A} \sigma_d(E_\gamma)\delta' \right] f(E_\gamma) \quad (1)$$

which takes into account the two possible mechanisms (i.e. photomeson and quasi-deuteron) discussed in the introductory section. In Eq. (1) A, Z, and N

represent the mass number, atomic number, and neutron number, respectively, of the target nucleus; $k(E_\gamma)$ is the ratio $\sigma_{\gamma A}/A\sigma_{\gamma N}$ which relates the γ -nucleus cross-section to the γ -nucleon cross section, and unity can be assumed at energies up to about 2 GeV (see Refs. 20, 21)^(*); δ and δ' are the factors related to the probability of nuclear excitation via the photomesonic and the quasi-deuteron primary interactions, respectively, and are both very close to unity for masses above 200 (Ref. 22); $\sigma_0(E_\gamma)$ is the total inelastic cross section of the interaction of a photon with a nucleon in the nucleus, corrected for the nucleon motion^(**), L is the Lvinger factor, whose value depends on the mass number of the nucleus and turns out to be about 12 for ^{209}Bi , ^{232}Th and ^{238}U ; $\sigma_d(E_\gamma)$ is the cross section of the photodisintegration of deuterium³; and $f(E_\gamma)$ is the fissility of the target nucleus, i.e. the ratio of the fission cross section σ_f to the total inelastic cross section σ_t . From the above listed considerations, Eq. (1) can be rewritten as

$$\sigma_f(E_\gamma) = \left[A\sigma_0(E_\gamma) + 12 \frac{NZ}{A} \sigma_d(E_\gamma) \right] f(E_\gamma). \quad (2)$$

To calculate $\sigma_f(E_\gamma)$, knowledge of the dependence of $f(E_\gamma)$ upon the target mass number A or the ratio Z^2/A and photon energy E_γ is essential, provided that the other parameters in Eq. (2) are known. Unfortunately, nuclear fissilities reported in literature up to now, do not cover the whole range of intermediate energies; moreover, the different values do not agree well with each other and are often mean values over a wide energy range. As a consequence, the

(*) A more detailed discussion about k can be found in Ref. 16.

(**) The more recent $\sigma_0(E_\gamma)$ values are those reported by Vartapetyan et. al. (see solid curve in Fig. 2 of the Ref. 16).

calculation of $f(E_\gamma)$ becomes indispensable.

Before entering into a detailed description of the calculation of nuclear fissilities, we believe it important to make a clear distinction between the probability of fission and fissility as considered in literature. Let us have the symbol f (the nuclear fissility of a nucleus), signify the above mentioned ratio. One can express σ_t in terms of the sum of a cross section σ_{nc} for the non compound nucleus (non-evaporative processes) and a cross section σ_c for the compound nucleus (fission-evaporation competition process); in other words

$$\sigma_t = \sigma_{nc} + \sigma_c . \quad (3)$$

The cross section σ_c is concerned with the de-excitation of the nucleus (A^*, Z^*) , that is, the final product of the cascade processes in the target nucleus (A, Z) .

Accordingly,

$$f = \frac{\sigma_f}{\sigma_{nc} + \sigma_c} . \quad (4)$$

A second quantity P_f must be introduced, which accounts for the probability that the nucleus (A^*, Z^*) will undergo fission; that is, P_f represents the ratio of the fission cross section to the compound nucleus cross section (excitation cross section) namely

$$P_f = \frac{\sigma_f}{\sigma_c} . \quad (5)$$

Of course this will result in a P_f larger than, or equal to, f . For sufficiently high bombarding energies σ_{nc} may be comparable to, or even greater than, σ_c and P_f may be considerable larger than f , whereas at intermediate energies σ_{nc} can be assumed small and P_f would not differ greatly from f .

In accordance with Eq. (2) the present calculation has been concerned with f .

III. THE CALCULATION OF NUCLEAR FISSION

Our intent in this section is to describe the basic assumption on which the calculation has been based and to show some details of the calculation itself.

One of the most serious troubles met in calculating photonuclear fission by means of the Monte Carlo Method is the lack of data on mass number A^* , atomic number Z^* , and excitation energy E^* of the residual nucleus of a photon-induced intranuclear cascade. The reason for this lack lies essentially in the enormous difficulty in carrying out the calculation of a cascade initiated by three particles (two photoproduced mesons and the recoil nucleon) at energies above 0.4 GeV. Gabriel and Alsmiller²³, in fact, reported photonuclear cross section data calculated up to 0.4 GeV, but there are no data for higher energies.

On the other hand, a number of Monte Carlo calculations on proton-induced intranuclear cascades have been published. We thought it feasible to use the well known $\langle A^* \rangle$ and $\langle Z^* \rangle$ average values from proton-initiated cascade data of Metropolis et al.²⁴ as a starting point for calculating the fission-evaporation competition at incident photon energies between 0.15 GeV and 2 GeV. Clearly, such a calculation would be valid for fission induced by protons only. However, Lindgren and Jonsson²⁵, in analysing their experimental results on photonuclear reactions in

iodine and gold by using the Rudstam's five parameters formula²⁶ in connexion with the Monte Carlo calculations of Gabriel and Alsmiller, concluded that although the primary interaction mechanisms are different, the average number of nucleons emitted in the fast cascade is almost the same for both proton- and photon-induced reactions. In addition, Roos and Peterson also found that the mean prong number of the stars in nuclear emulsions was essentially independent of the nature of the bombarding particle and was a function of the available energy. These arguments confirmed our idea of applying the proton data to the calculation of f , regardless of the kind of incident particle.

The following are basic assumptions that we have used in our calculation:

(i) The mass number A^* and the atomic number Z^* of the residual post-cascade nucleus are given by

$$\begin{aligned} A^* &= A - \Delta A \\ Z^* &= Z - \Delta Z \end{aligned} \tag{6}$$

where A and Z refer to the target nucleus and ΔA and ΔZ are the number of nucleons and protons lost in the cascade, respectively. Both ΔA and ΔZ were chosen at random from the following distribution curve

$$N(x)dx = C x^2 \exp(-3x/\bar{x})dx, \quad x \geq 0 \tag{7}$$

where $x = \Delta A$ or ΔZ , C is a constant, and \bar{x} the mean value of x . The distribution given by Eq. (7) was chosen in such a way that it agreed, at least formally, with the results obtained by other authors^{24, 27, 28}. Although other

similar distributions are possible, Eq. (7) is the easiest to handle in the calculation and it was centered around the mean values of ΔA and ΔZ taken from the work of Metropolis et al²⁴.

(ii) The excitation energy E^* was obtained randomly from a distribution curve of the type

$$N(U)dU = C'U \exp(-2U/\bar{U})dU, \quad 0 \leq U \leq \bar{U} \quad (8)$$

$$N(U)dU = 0, \quad U > \bar{U}$$

where $U = E^*$, C' is a constant, and \bar{U} the mean value of U . For incident energies E_i smaller than the binding energy B^* of the residual nucleus (A^* , Z^*), the excitation energy distribution covers the range $0 \leq E^* \leq E_i$, while for incident energies larger than B^* it covers the range $0 \leq E^* \leq B^*$; this latter condition arising from nuclear stability considerations. Thus the excitation energy distribution given by Eq. (8) was used with the following conditions.

$$\bar{U} = E_i, \quad E_i \leq B^* \quad (9)$$

$$\bar{U} = B^*, \quad E_i > B^*$$

Also in this case the choice of Eq. (8) was made in such a manner that it agreed formally with the distributions given by different authors for incidente protons^{24,29}.

The de-excitation of the residual nucleus was then treated as a competition between particle evaporation and fission, in a manner similar to that described by Dostrovsky et al³⁰. We took into consideration the evaporation of

neutrons, protons, deuterons, tritons, ${}^3\text{He}$ and ${}^4\text{He}$. The separation energies for these particles were calculated by means of the semi-empirical mass formula, using the binding energy values for the different charged particles given in the compilation of nuclear masses of Mattauch et al.³¹. The parameters used for the coefficients in the mass formula were those of Nix and Sassi³², corresponding to $r_0 = 1.216$ fermi. Coulomb barriers for the different charged particles were corrected for the tunnel effect and nuclear temperature T , as indicated by Le Couteur³³ and Fujimoto and Yamaguchi³⁴, respectively. The probability of fission relative to neutron emission has been introduced in the same manner as in Ref. 30. The fission barriers B_f have been calculated by means of the Liquid Drop Model, taking into account the effect of neutron excess³⁵ and corrected for nuclear temperature, as in the case of Coulomb barriers, that is

$$B_f(T) = B_{f_0} (1 - T^2/T_c^2) \quad (10)$$

T_c is the critical nuclear temperature (≈ 9 MeV) i.e. the temperature at which surface tension vanishes. The energy distribution of the evaporated particles was assumed to obey the Weisskopf' distribution³⁶, and a level-density parameter $a = A/10 \text{ MeV}^{-1}$ was used.

Using the IBM/370 computer of the CBPF the calculation has been performed for five energies of the incident photon, between 0.15 GeV and 2 GeV, on ${}^{209}\text{Bi}$, ${}^{232}\text{Th}$, and ${}^{238}\text{U}$. The treatment in each case (fixed incident energy and target nucleus) involved about 500 iterations. The input data included E_i , A , Z , $\langle\Delta A\rangle$, $\langle\Delta Z\rangle$. The residual nucleus (A^*, Z^*) was chosen by means of two number from a uniformly distributed random number in the interval 0 to 1, using the ΔA and ΔZ distribution given by Eq. (7). A third random number was used

to obtain E^* from Eq. (8), with the restrictions imposed by Eq. (9). The probabilities of fission and particle evaporation were computed as in Ref. 30. From the cumulative sums of these probabilities, normalized to a total of 1, either the particle to be evaporated or fission was chosen using another random number. Accordingly, the kinetic energy of the emitted particle (if emission occurred), was selected from a Weisskopf' kinetic energy distribution for the appropriate temperature, using a random number. The iteration was continued until the initial excitation energy was almost entirely removed, i.e. until the excitation energy was so low that neither particle evaporation nor fission could take place. The nuclear fissility at each energy and for a given nucleus has been obtained from the ratio of the number of cases for which fission took place to the total number of iterations.

The present calculation differs from other similar ones in some important aspects. It takes into consideration the evaporation of six kinds of particles and distributions of ΔA , ΔZ and E^* while Nix and Sassi³² considered only the evaporation of neutrons and protons and the average values of ΔA , ΔZ and E^* . Finally, an energy dependence of the ratio of the neutron emission width to fission width has been taken into consideration, whereas in Ref. 37 this ratio was assumed to be independent of the energy.

IV. RESULTS AND DISCUSSION

The results of the calculation are shown in Fig. 1 and Fig. 2. Fig. 1 reports fissility values for ^{238}U as a function of the incident energy. In this figure the results of Hahn and Bertini³⁷ for the same nucleus are reported for comparison (broken lines). As one can see, the present values agree quite satisfactorily with those calculated by Hahn and Bertini for incident protons. Fig. 2

shows the results obtained in the present calculation for ^{209}Bi , ^{232}Th and ^{238}U and a comparison has been made with the more recent experimental data on proton fissilities of Nazareth³⁸ (dashed curves). Good agreement is found for ^{238}U and ^{209}Bi , though at the lower energies the agreement fails for ^{232}Th .

A comparison among calculated fissilities and the experimental values for incident photons is shown in Figs. 3 and 4 and in Tables I and II. In Fig. 3 the nuclear fissility f is plotted against the incident photon energy. The calculated average \bar{f} values in the energy range 0.3-1 GeV are 0.8, 0.6 and 0.1 for ^{238}U , ^{232}Th and ^{209}Bi , respectively. These values show almost complete agreement with the experimental values 0.84 (Ref. 7) and 0.8 (Ref. 13) for ^{238}U , 0.62 (Ref. 11) and 0.6 (Ref. 13) for ^{232}Th , and 0.12 (Ref. 6) for ^{209}Bi . Disagreement is found with the experimental value of Jungerman and Steiner⁵ for ^{209}Bi , which is about twice the average value of the present calculation, in the range 0.15-0.5 GeV, and with that of Carbonara et al.⁷ for ^{232}Th in the range 0.3-1 GeV. Tables I and II report all existing experimental data on f and P_f , respectively, for the nuclei considered in the present work, at photon energies between 0.2 GeV and 1 GeV. In Table II the present work values of P_f have been calculated by means of Eq. (5) using the nuclear transparencies given in Ref. 22.

Fig. 4 is a plot of the fissilities of nuclei ranging between ^{181}Ta and ^{238}U as functions of the Z^2/A ratio^(*), at a photon energy of 0.35 GeV

(*) Strictly speaking, the ratio to be considered here would be $(Z^*)^2/A^*$ for the fissioning excited nucleus. It is customary, however, to refer to the Z^2/A of the target nucleus, and we agreed with this convention.

(this value corresponds roughly to the abscissa of the first pion resonance, where most of experimental photofission cross section curves show maxima). The straight line in the figure is achieved by using the least-squares method for all the experimental f values. The graph reports P_f values as well as our results for the sake of comparison. Also in this case, the calculated fissilities agree almost completely with the slope of the straight line, only the ^{232}Th fissility being somewhat higher (the calculation of Nix and Sassi³², however, gives values very close together for ^{232}Th and ^{238}U fissilities).

The general trend of the curves in Figs. 1 and 2 can be explained in the following way. At energies between 0.15 GeV and 0.6 GeV, the post-cascade nucleus has a low excitation energy and emission of neutrons is therefore favoured with respect to protons and heavier charged particles. This corresponds to an increase of the Z^2/A ratios of the residual nuclei and hence to a decrease in fission barriers. As a consequence, fissility will be enhanced. Above 0.6 GeV, the highly excited nucleus evaporates a large number of charged particles, because of the smaller value of the Coulomb barrier caused by the increase in nuclear temperature. The residual nuclei have smaller Z^2/A ratios and higher fission barriers, with the consequence that nuclear fissility decreases for the nuclei we considered.

In calculating the photofission cross sections, use has been made of Eq. (2) with the values of nuclear fissility which we obtained. It has already been pointed out that Eq. (2) accounts for both the photomeson and the quasi-deuteron models. Moretto et al.⁹, in analysing their results from electron- and bremsstrahlung-induced fission in different nuclei, assumed that in the energy region 0.2- 0.4 GeV, the probability of photoproduced pions leaving the nucleus without interaction is great and **therefore** the photomeson excitation process is

ineffective in giving the nucleus sufficiently high excitation energy for fission to occur, especially in the case of medium-heavy nuclei such as ^{209}Bi . They concluded that for such nuclei the quasi-deuteron process is solely responsible for fission; and for heavier nuclei, this process dominates. On the other hand several authors^{4, 12-16} tend to ascribe a predominant role in nuclear excitation to the photomeson processes. There are various arguments which make the conclusions of Moretto et al.⁹ hardly acceptable; (i) owing to the smallness of the deuteron photodisintegration cross section in this energy range, very high fissilities would be required to make photofission cross sections comparable with those experimentally determined; (ii) there is no reason why a photon should be more efficient than a proton in producing highly excited nuclei with the mechanism of the quasi-deuteron interaction; (iii) the transparencies for photoproduced pions are not so high as to justify the assumption of a negligible contribution from the photomeson processes (for π^0 -mesons, transparencies of ^{209}Bi have been calculated²² of 0.50 at $E_\gamma = 0.2$ GeV and 0.03 at $E_\gamma = 0.3$ GeV). In order to remove this ambiguity to some extent, we calculated $\sigma_f(E_\gamma)$ in a still different manner, i.e. by means of the formula

$$\sigma_f(E_\gamma) = A\sigma_0(E_\gamma) f(E_\gamma) \quad (11)$$

which accounts for the photomeson mechanism only, thus disregarding the quasi-deuteron contribution.

Fig. 5 and 6 show the results of such calculations, based on both Eq. (2) and Eq. (11). In the figures, the calculated photofission cross section has been plotted as a function of the incident photon energy and experimental curves have been reported to allow a comparison. At first glance, the calculated

trends which seem to agree best with the experimental data for ^{209}Bi and ^{232}Th are those arising from Eq. (11) (photomeson only, solid curves). For ^{238}U the situation is less clear, taking in consideration the much larger differences that exist among the experimental curves. For instance, at an incident energy of 0.3 GeV, a cross section of 110 mb has been reported by Wakuta¹⁴ for ^{238}U (dot-dashed line), whereas other authors have found much lower values. Probably Wakuta's cross sections for ^{238}U are somewhat too high.

Two sets of data show very good agreement with the present results; the experimental data of Methasiri¹³ and the calculated data by Vartapetyan et al.¹⁶, although Methasiri's curves do not exhibit bumps in the region of the second meson resonance. Taking the respective errors and uncertainties into account, the agreement with the estimated curves of Vartapetyan et al. (dot-dashed, Fig. 6) is practically complete at energies up to 1 GeV. These data and ours strongly support the photomeson model of initial interaction. The present calculation clearly shows that the photomeson contribution to σ_f , as calculated with Eq. (2), varies from a minimum of 50 percent at 0.2 GeV to a maximum of 80 percent at 0.4 GeV. Thus we are led conclude that photomeson processes contribute to a very large extent to σ_f in medium-heavy nuclei and that they are predominant in heavy nuclei.

This is in sharp contradiction to the conclusions of Moretto et al.⁹. The reason for this discrepancy may be that in their work Moretto et al. used electron excitation and a theoretical virtual-photon spectrum was employed in deducing photofission cross sections and fission probabilities. Due to the uncertainty of this method, large systematic errors might be introduced in processing the experimental yields, and in such a way find the extraordinarily high P_f values for ^{209}Bi and ^{208}Pb (see Fig. 4) an explanation.

trends which seem to agree best with the experimental data for ^{209}Bi and ^{232}Th are those arising from Eq. (11) (photomeson only, solid curves). For ^{238}U the situation is less clear, taking in consideration the much larger differences that exist among the experimental curves. For instance, at an incident energy of 0.3 GeV, a cross section of 110 mb has been reported by Wakuta¹⁴ for ^{238}U (dot-dashed line), whereas other authors have found much lower values. Probably Wakuta's cross sections for ^{238}U are somewhat too high.

Two sets of data show very good agreement with the present results; the experimental data of Methasiri¹³ and the calculated data by Vartapetyan et al.¹⁶, although Methasiri's curves do not exhibit bumps in the region of the second meson resonance. Taking the respective errors and uncertainties into account, the agreement with the estimated curves of Vartapetyan et al. (dot-dashed, Fig. 6) is practically complete at energies up to 1 GeV. These data and ours strongly support the photomeson model of initial interaction. The present calculation clearly shows that the photomeson contribution to σ_f , as calculated with Eq. (2), varies from a minimum of 50 percent at 0.2 GeV to a maximum of 80 percent at 0.4 GeV. Thus we are led conclude that photomeson processes contribute to a very large extent to σ_f in medium-heavy nuclei and that they are predominant in heavy nuclei.

This is in sharp contradiction to the conclusions of Moretto et al.⁹. The reason for this discrepancy may be that in their work Moretto et al. used electron excitation and a theoretical virtual-photon spectrum was employed in deducing photofission cross sections and fission probabilities. Due to the uncertainty of this method, large systematic errors might be introduced in processing the experimental yields, and in such a way find the extraordinarily high P_f values for ^{209}Bi and ^{208}Pb (see Fig. 4) an explanation.

A comparison between the present calculation and the experimental data of de Carvalho et al.⁶, Carbonara et al.⁷, and Emma et al.¹⁷ may be very useful. These authors measured average photofission cross sections in the energy range 0.3-1 GeV; consequently a comparison can be made only with the average values of σ_f , which were easily calculated from Eq. (2) and Eq. (11) in the same energy range. Table III reports these average values. The three sets of experimental data are somewhat higher than our calculated values. In deducing fissilities, de Carvalho et al. and Carbonara et al. derived the average total reaction cross sections by means of the formula $\bar{\sigma}_t = A\bar{\sigma}_0$, with $\bar{\sigma}_t$ and $\bar{\sigma}_0$ standing for the average values of σ_t and σ_0 in the energy range 0.3-1 GeV, σ_0 having been corrected for the Fermi momentum of the nucleon. They assumed $\bar{\sigma}_0 = (335 \pm 40) \mu\text{b}$, following Castagnoli et al.³⁹ and Roos and Peterson. Recent more accurate measurements^(*) give $\bar{\sigma}_0 = 256 \mu\text{b}$. With this latter value one obtains the following values of $\bar{\sigma}_t$: 61mb, 59mb, and 54mb for ^{238}U , ^{232}Th , and ^{209}Bi , respectively. The fissilities given by de Carvalho et al. and Carbonara et al. must therefore be increased to 0.14 for ^{209}Bi , 0.63 for ^{232}Th , and 1.1 for ^{238}U , which indicates that $\bar{\sigma}_f$ of ^{238}U is rather overestimated. With this correction, agreement is found with the ^{209}Bi and ^{232}Th photofission cross sections and fissilities of de Carvalho et al.⁶ and Carbonara et al.⁷. The results of Emma et al.¹⁷ for ^{209}Bi also agree with ours within the limits of errors.

V. SUMMARY

In concluding this paper we wish to point out some important

(*) See footnote on page 71.

results. The calculated fissilities are in good agreement with most of the values obtained in experiments using photons. This seems to support the point of view that nuclear excitation does not depend on a particular kind of bombarding particle, but depends only on the incident energy (available energy), at least for medium-heavy nuclei^(*).

The trend of the photofission cross section turns out to be strictly connected to the photomeson mechanism of nuclear excitation, even though the quasi-deuteron mechanism may give some contribution in the energy region 0.15-0.50 GeV.

Since fission represents a large contribution to the total inelastic cross section for the heaviest nuclei, photofission experiments at the higher energies will clarify some scarcely known aspects of photon interaction, such as the seemingly hadronic behavior of high-energy photons.

(*) In this region of nuclear masses, the Z^2/A dependence of nuclear fissility is approximately the same for photons, protons, and α -particles (in the lighter nuclei, however, this similarity no longer subsists for the α -particles). A quite different trend seems to be exhibited by the ^{16}O -induced fission, for which fissilities are remarkably higher than for smaller particles, also in the medium-heavy region of masses (see Ref. 18).

TABLE I. Nuclear fissilities for ^{209}Bi , ^{232}Th , and ^{238}U from photofission data.

Nucleus	Photon energy (GeV)									Method	
	0.20	0.30	0.35	0.40	0.45	0.50	0.65	0.80	1.00		
^{209}Bi	0.25	0.25									Nucl.Emulsion ^a
	0.15	0.15	0.15	0.15	0.15	0.15					Ioniz.Chamber ^b
		0.12	0.12	0.12	0.12	0.12	0.12	0.12	0.12		Nucl.Emulsion ^c
		0.10	0.11	0.12	0.15	0.16	0.17	0.19	0.20		Glass Detector ^d
		0.07	0.10	0.11	0.11	0.11	0.11	0.11	0.10		Calculation ^e
^{232}Th	0.50	0.50	0.50	0.50	0.50	0.50					Ioniz.Chamber ^b
		0.47	0.47	0.47	0.47	0.47	0.47	0.47	0.47		Nucl.Emulsion ^f
			0.60								Glass Detector ^g
	0.78	0.81	0.81	0.80	0.80	0.78	0.67	0.52	0.41		Calculation ^e
^{238}U	0.50	0.50	0.50	0.50	0.50	0.50					Ioniz.Chamber ^b
		0.84	0.84	0.84	0.84	0.84	0.84	0.84	0.84		Nucl.Emulsion ^f
			0.80								Glass Detector ^g
								1.04	1.04		Mica Detector ^h
	0.9	0.92	0.91	0.91	0.90	0.88	0.81	0.70	0.50		Calculation ^e

^aG. Bernardini, R. Reitz, and E. Segré, Phys. Rev. 90, 573 (1953).

^bJ.A. Jungerman and H.M. Steiner, Phys. Rev. 106, 585 (1957).

^cH.G. de Carvalho, G. Cortini, E. del Giudice, G. Potenza, R. Rinzi, and G. Ghigo, Nuovo Cim. 32, 293 (1964).

^dG.A. Vartapetyan, N.A. Demekhina, V.I. Kasilov, Yu.N. Ranyuk, P.V. Sorokin, and A.G. Khudaverdyan, Kharkov Physical Technical Institute, Report No. KPTI 70-27 (unpublished).

^eMethod of calculation described in text.

^fF. Carbonara, H.G. de Carvalho, R. Rinzi, E. Sassi, and G.P. Murtas, Nucl.Phys. 73, 385(1965).

^gT. Methasiri, Nucl. Phys. A158, 433 (1970).

^hP. David, J. Debrus, U. Kim, G. Kumbartzki, H. Mommsen, W. Soye, K.H. Speidel, and G. Stein, Nucl. Phys. A197, 163 (1972).

TABLE II. Fission probabilities for ^{209}Bi , ^{232}Th , and ^{238}U from photofission data.

Nucleus	Photon energy (GeV)									Method
	0.20	0.30	0.35	0.40	0.45	0.50	0.65	0.80	1.00	
^{209}Bi	0.10	0.30	0.40	0.60	0.90					Mica Detector ^a
	0.08	0.12	0.13	0.14	0.14	0.14	0.14	0.13	0.12	Calculation ^b
^{232}Th	0.16	0.25	0.39	0.58	0.74	0.40	0.40	0.40	0.40	Calculation ^c
		0.38	0.38	0.38	0.38	0.38				Semi-Cond. Detec. ^d
	0.86	0.88	0.88	0.87	0.85	0.82	0.63	0.52	0.44	Calculation ^b
^{238}U	0.40	0.46	0.56	0.68	0.79	0.40	0.40	0.40	0.40	Calculation ^c
	0.80	0.80	0.80	0.80	0.80	0.80	0.80	0.80		Mica Detector ^a
		1.00	1.00	1.00	1.00	1.00				Semi-Cond. Detec. ^d
	0.93	0.95	0.94	0.93	0.92	0.90	0.80	0.63	0.51	Calculation ^b

^aL.G. Moretto, R.C. Gatti, S.G. Thompson, J.T. Routti, J.H. Heisenberg, L.M. Middleman, M.R. Yearian, and R. Hofstadter, Phys. Rev. 179, 1176 (1969).

^bCalculated values according to Eq. (5).

^cB. Schröder, G. Nydahl, and B. Forkman, Nucl. Phys. A143, 449 (1970).

^dY. Wakuta, J. Phys. Soc. Japan 31, 12 (1971).

TABLE III. Average values of the photofission cross section in the energy range 0.3-1 GeV.

Target nucleus	Cross section (mb)	
	Calculated	Experimental
^{209}Bi	6.1 ^a	7.8 ± 0.8^c
	5.6 ^b	7.6 ± 0.2^d
^{232}Th	43 ^a	37 ± 4^e
	38 ^b	
^{238}U	52 ^a	67 ± 7^e
	47 ^b	

^aCalculated value according to Eq. (2).

^bCalculated value according to Eq. (11).

^cH.G. de Carvalho, G. Cortini, E. Del Giudice, G. Potenza, R. Rinzi-
villo, and G. Ghigo, *Nuovo Cim.* 32, 293 (1964).

^dV. Emma, S. Lo Nigro, and C. Milone, *Lett. Nuovo Cim.* 2,
117 (1971).

^eF. Carbonara, H.G. de Carvalho, R. Rinzi-
villo, E. Sassi, and G.P. Murtas, *Nucl. Phys.* 73, 385 (1965).

FIGURE CAPTIONS

- Fig. 1. Calculated nuclear fissility for ^{238}U . The smoothed curve is an eye fit to the present calculated points; errors in the calculations are statistical uncertainties of the Monte Carlo computations. The broken lines are the results from Ref. 37; the lower broken line (-.-.-) is referred as that agreeing with most of the experimental data from proton-induced fission.
- Fig. 2. Nuclear fissility for ^{209}Bi , ^{232}Th , and ^{238}U . The solid curves are eye fits to the present calculated points; errors in the calculations are statistical uncertainties of the Monte Carlo computations. The dashed curves are experimental results from Ref. 38 for proton-induced fission.
- Fig. 3. Nuclear fissility for ^{209}Bi , ^{232}Th , and ^{238}U . The solid curves are the results of the present calculations. Experimental fissility values are taken from: Ref. 7 (---- for U), Ref. 13 (Δ for U), Ref. 11(.... for Th) Ref. 13 (\blacktriangle for Th), Ref. 7 (--- for Th), Ref. 5 (-.-.- for Bi), and Ref. 6 (-.-.- for Bi).
- Fig. 4. Nuclear fissility for nuclei ranging from ^{181}Ta to ^{238}U versus the Z^2/A ratio at 0.35 GeV photon energy. Present calculations (\blacktriangledown). Experimental data are taken from: Ref. 5 (\blacksquare), Refs. 6 and 7 (\blackstar), Ref. 11 (0), Refs. 13 and 15 (Δ); the straight line is a least-squares fit of the experimental points only. To allow a comparison the experimental fission

probabilities (at 0.35 GeV) are also shown; data are taken from: Ref. 9 (\square) Ref. 12 (\bullet), and Ref. 14 (\blacktriangle).

Fig. 5. Photofission cross section versus incident photon energy for ^{209}Bi (a), ^{232}Th (b), and ^{238}U (c). The solid curves are the results obtained by means of Eq. (11); the dashed curves are the results obtained by means of Eq. (2). In Fig. 5(a) the experimental data are taken from Ref. 5(-.-.-), and in Figs. 5(b) and (c) the experimental data are taken from Ref. 13 (-.-.-.-) and Ref. 14 (-.-.-).

Fig. 6. Photofission cross section versus incidente photon energy for ^{209}Bi (a), ^{232}Th (b), and ^{238}U (c). The solid curves are the results obtained by means of Eq. (11); the dashed curves are the results obtained by means of Eq. (2); the dot-dashed curves are the estimates from Ref. 16. In Fig. 6(a) the curve marked q-d has been obtained by subtracting Eq. (11) from Eq. (2) and represents the contribution of the primary quasi-deuteron interaction (for the sake of simplicity, this contribution has been shown in Fig. 6 (a) only). The experimental data in Fig. 6(a) are taken from Ref. 6 (-.-.-.-) and Ref. 17 (.....); the experimental data in Figs. 6(b) and (c) are taken from Ref. 7 (-.-.-.-).

ACKNOWLEDGMENTS

The authors wish to thank Prof. F. Salvetti for useful discussion on this subject. J.B. Martins and O.A.P. Tavares wish to thank the "Istituto di Chimica Generale ed Inorganica dell'Università di Roma" for the very kind hospitality they received during the preparation of the manuscript.

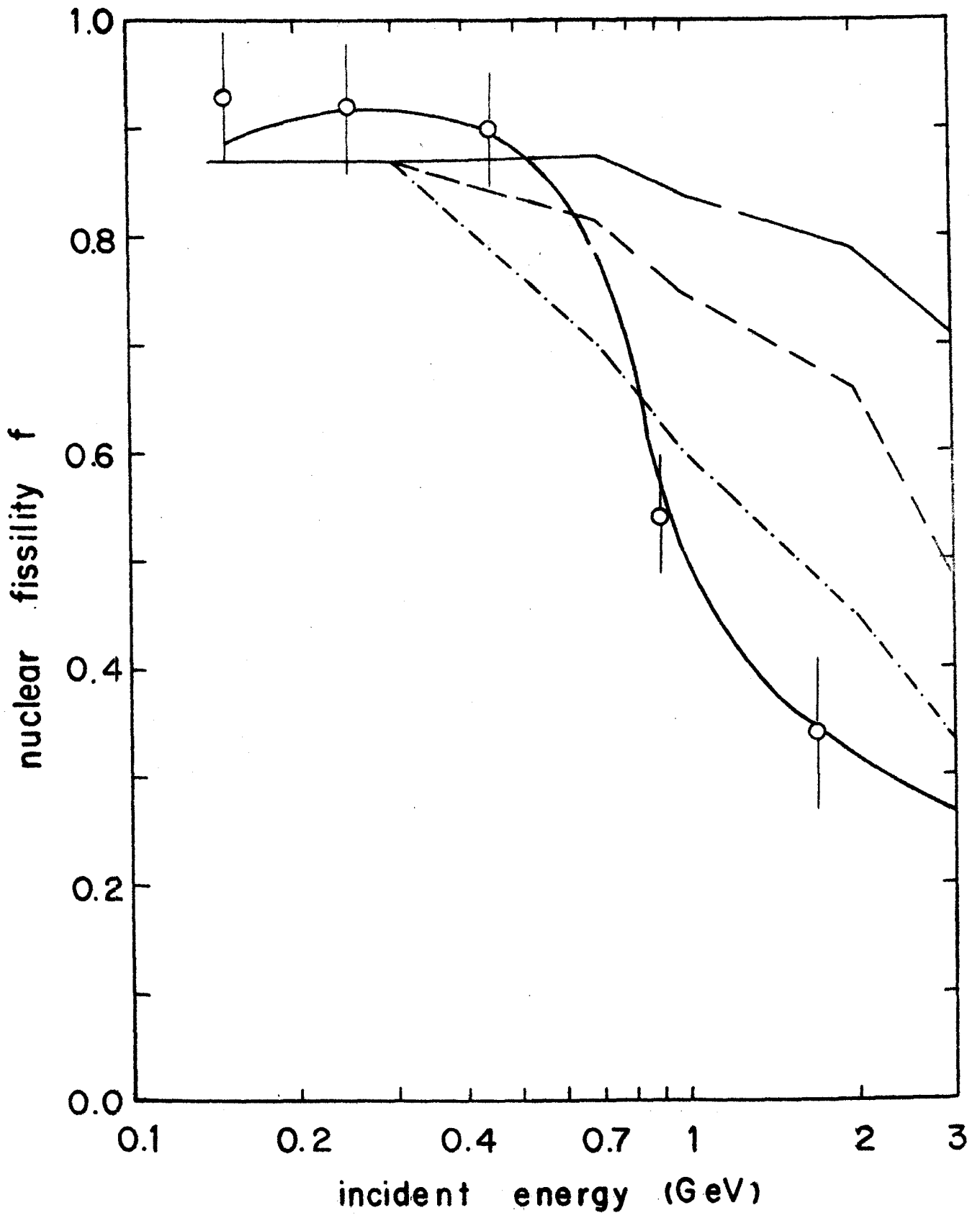


FIG.1

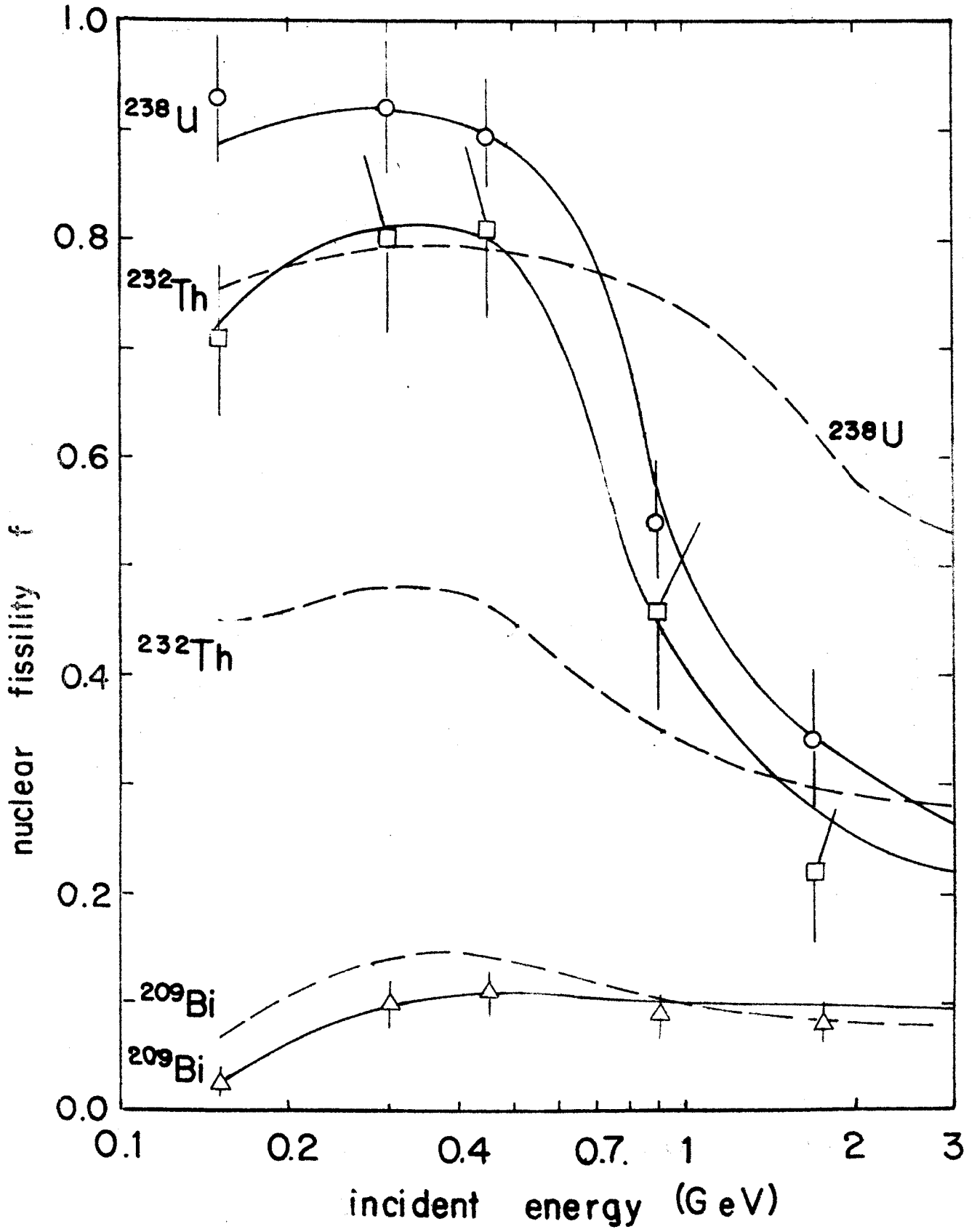


FIG.2

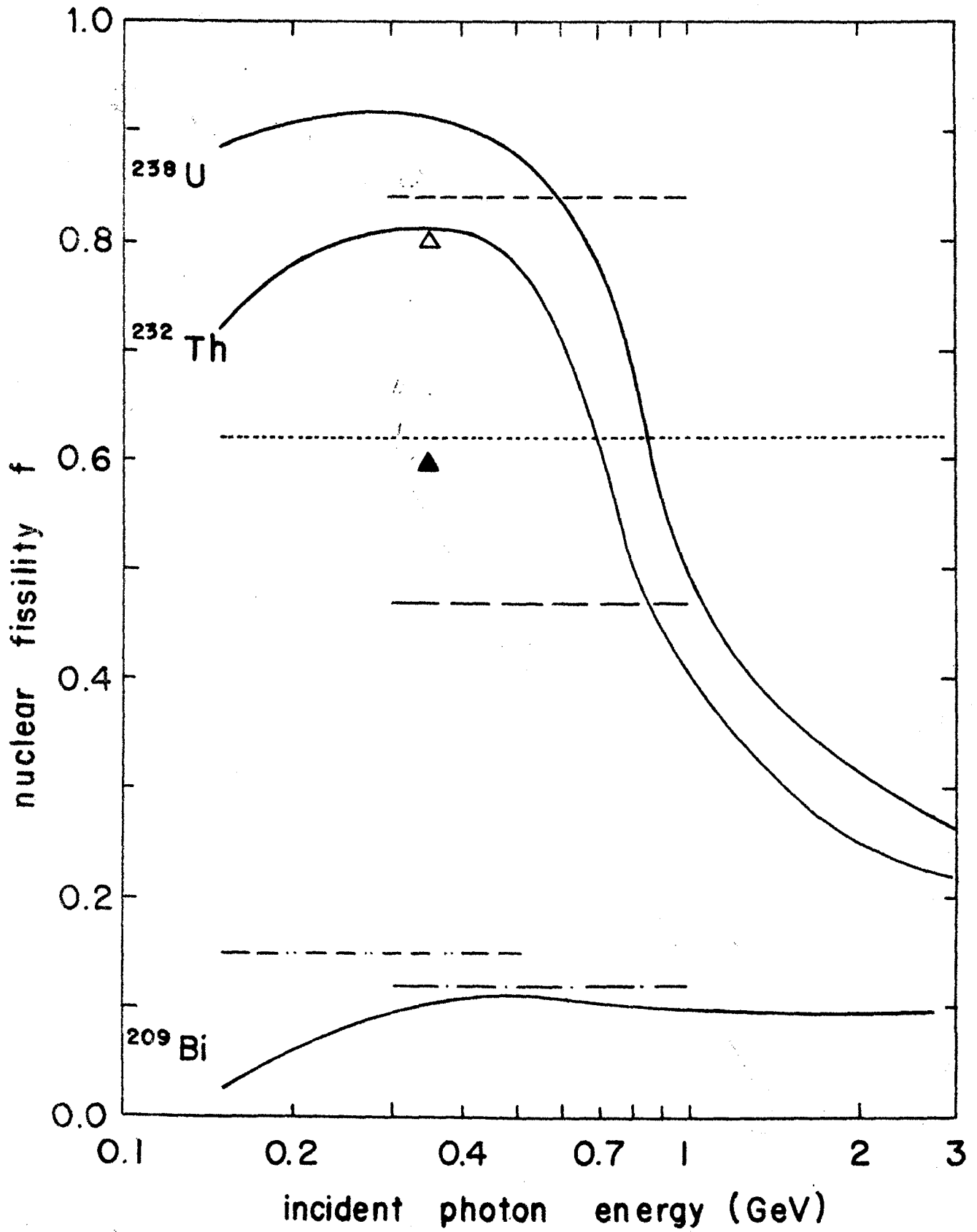


FIG. 3

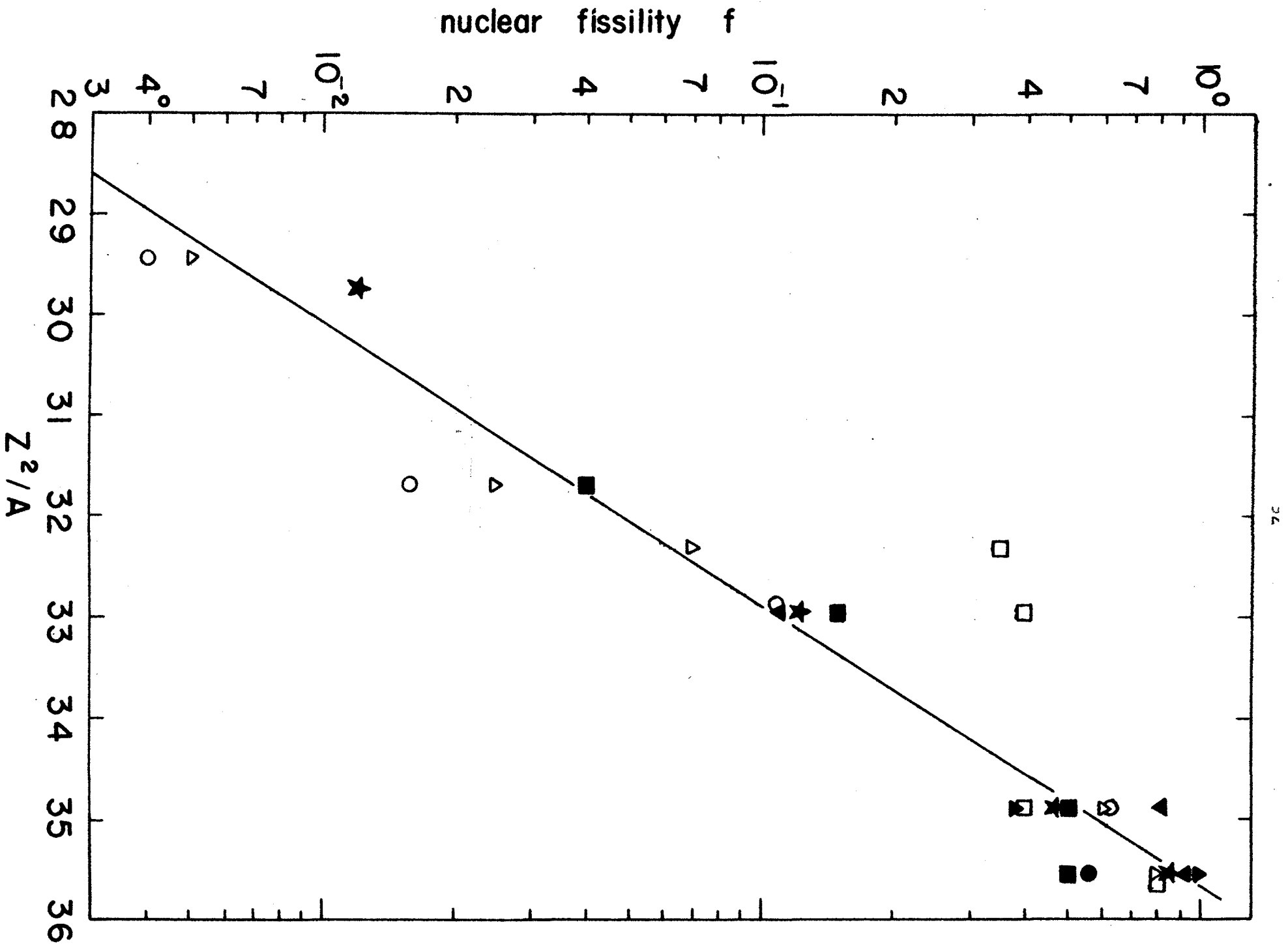


FIG. 1

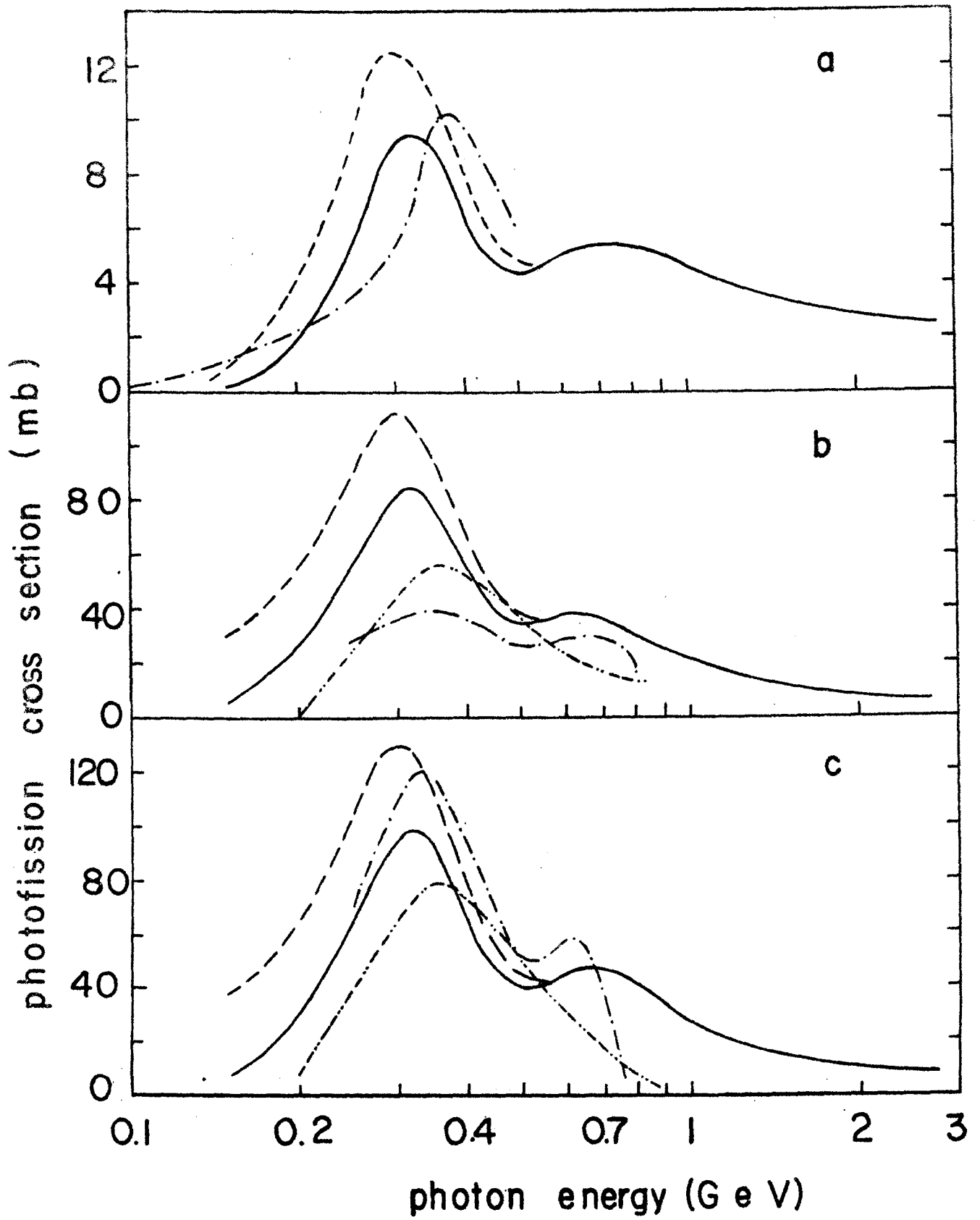


FIG.5

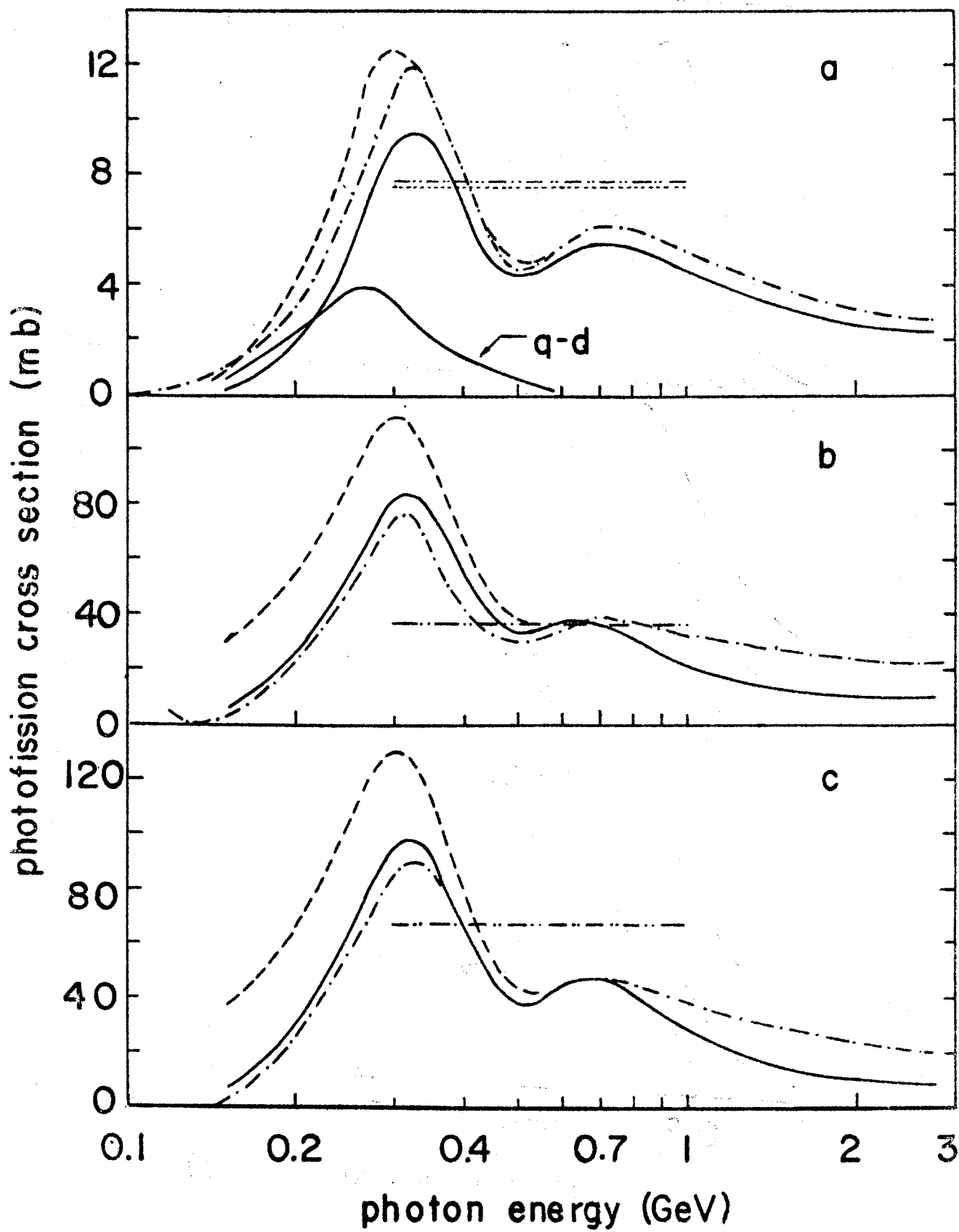


FIG. 6

REFERENCES

1. R. Serber, Phys. Rev. 72, 1114 (1943).
2. I. Reff, Phys. Rev. 91, 150 (1953).
3. J.S. Levinger, Phys. Rev. 84, 43 (1951); 97, 970 (1955).
4. G. Bernardini, R. Reitz, and E. Segré, Phys. Rev. 90, 573 (1953).
5. J.A. Jungerman and H.M. Steiner, Phys. Rev. 106, 585 (1957).
6. H.G. de Carvalho, G. Cortini, E. del Giudice, G. Potenza, R. Rinzivillo, and G. Ghigo, Nuovo Cim. 32, 293 (1964).
7. F. Carbonara, H.G. de Carvalho, R. Rinzivillo, E. Sassi, and G.P. Murtas, Nucl. Phys. 73, 385 (1965).
8. A.V. Mitrofanova, Yu. N. Ranyuk, and P.V. Sorokin, Sov. J. Nucl. Phys. 6, 512 (1968).
9. L.G. Moretto, R.C. Gatti, S.G. Thompson, J.T. Routti, J.H. Heisenberg, L.M. Middleman, M.R. Yearian, and R. Hofstadter, Phys. Rev. 179, 1176 (1969).
10. Y. Wakuta, M. Sonoda, A. Katase, H. Tawara, and M. Hyakutake, J. Phys. Soc. Japan 26, 851 (1969).
11. G.A. Vartapetyan, N.A. Demekhina, V.I. Kasilov, Yu. N. Ranyuk, P.V. Sorokin, and A.G. Khudaverdyan, Kharkov Physical Technical Institute, Report. No. KPTI 70-27 (unpublished).
12. B. Schröder, G. Nydahl, and B. Forkman, Nucl. Phys. A143, 449 (1970).
13. T. Methasiri, Nucl. Phys. A158, 433 (1970).
14. Y. Wakuta, J. Phys. Soc. Japan 31, 12 (1971).
15. T. Methasiri and S.A.E. Johansson, Nucl. Phys. A167, 97 (1971).
16. G.A. Vartapetyan, N.A. Demekhina, V.I. Kasilov, Yu. N. Ranyuk, P.V. Sorokin, and A.G. Khudaverdyan, Yad. Fiz. 14, 65 (1971); [translation: Soviet J. Nucl. Phys. 14, 37 (1972)]

17. V. Emma, S. Lo Nigro, and C. Milone, *Lett. Nuovo Cim.* 2, 117 (1971).
18. B. Forkman and B. Schröder, *Phys. Scripta* 5, 105 (1972).
19. P. David, J. Debrus, U. Kim, G. Kumbartzki, H. Mommsen, W. Soyez, K.H. Speidel, and G. Stein, *Nucl. Phys.* A197, 163 (1972); P. David, J. Debrus, F. Lübke, H. Mommsen, R. Schoenmackers, and G. Stein, *Proceedings of the International Conference on Photonuclear Reactions and Applications* (Pacific Grove, 1973), Session 8C6.
20. S.J. Brodsky and J. Pumplin, *Phys. Rev.* 182, 1794 (1969).
21. D.O. Caldwell, V.B. Elings, W.P. Hesse, G.E. Jahn, R.J. Morrison, F.K. Murphy, and D.E. Yount, *Phys. Rev. Letters* 23, 1256 (1969).
22. H.G. de Carvalho, J.B. Martins, O.A.P. Tavares, R.A.M.S. Nazareth, and V. di Napoli, *Lett. Nuovo Cim.* 2, 1139 (1971); 4, 365 (1972).
23. T.A. Gabriel and R.G. Alsmiller, *Phys. Rev.* 182, 1035 (1969).
24. N. Metropolis, R. Bivins, M. Storm, A. Turkevich, and G. Friedlander, *Phys. Rev.* 110, 185 (1958); N. Metropolis, R. Bivins, M. Storm, J.M. Miller, G. Friedlander, and A. Turkevich, *Phys. Rev.* 110, 204 (1958).
25. K. Lindgren and G.G. Jonsson, *Nucl. Phys.* A197, 71 (1972).
26. G. Rudstam, *Z. Naturforsch* 21a, 1027 (1966).
27. G. Rudstam, Ph. D. thesis, University of Uppsala, 1956 (unpublished).
28. J.W. Meadows, *Phys. Rev.* 98, 744 (1955).
29. V.S. Barashenkov, H.W. Bertini, K. Chen, G. Friedlander, G.D. Harps, A.S. Ilginov, S.M. Miller, and V.D. Toneev, *Nucl. Phys.* A187, 531 (1972).
30. I. Dostrovsky, P. Rabinowitz, and R. Bivins, *Phys. Rev.* 111, 1659 (1958); I. Dostrovsky, Z. Fraenkel, and P. Rabinowitz, in *Proceedings of the Second United Nations Conference on the Peaceful Uses of Atomic Energy* (United Nations, Geneva, 1958), vol. 15P/1615.